ChemPubSoc
Europe

■ **Fullerenes** |*Hot Paper*|

Fullerene Building Blocks with Tailor-Made Solubility and New Insights into Their Hierarchical Self-Assembly

M. Eugenia Pérez-Ojeda,[a] Isabell Wabra,[a] Christoph Böttcher,[b] and Andreas Hirsch*[a]

Dedicated to the memory of my father, C. N. Eugenio Pérez-Ojeda
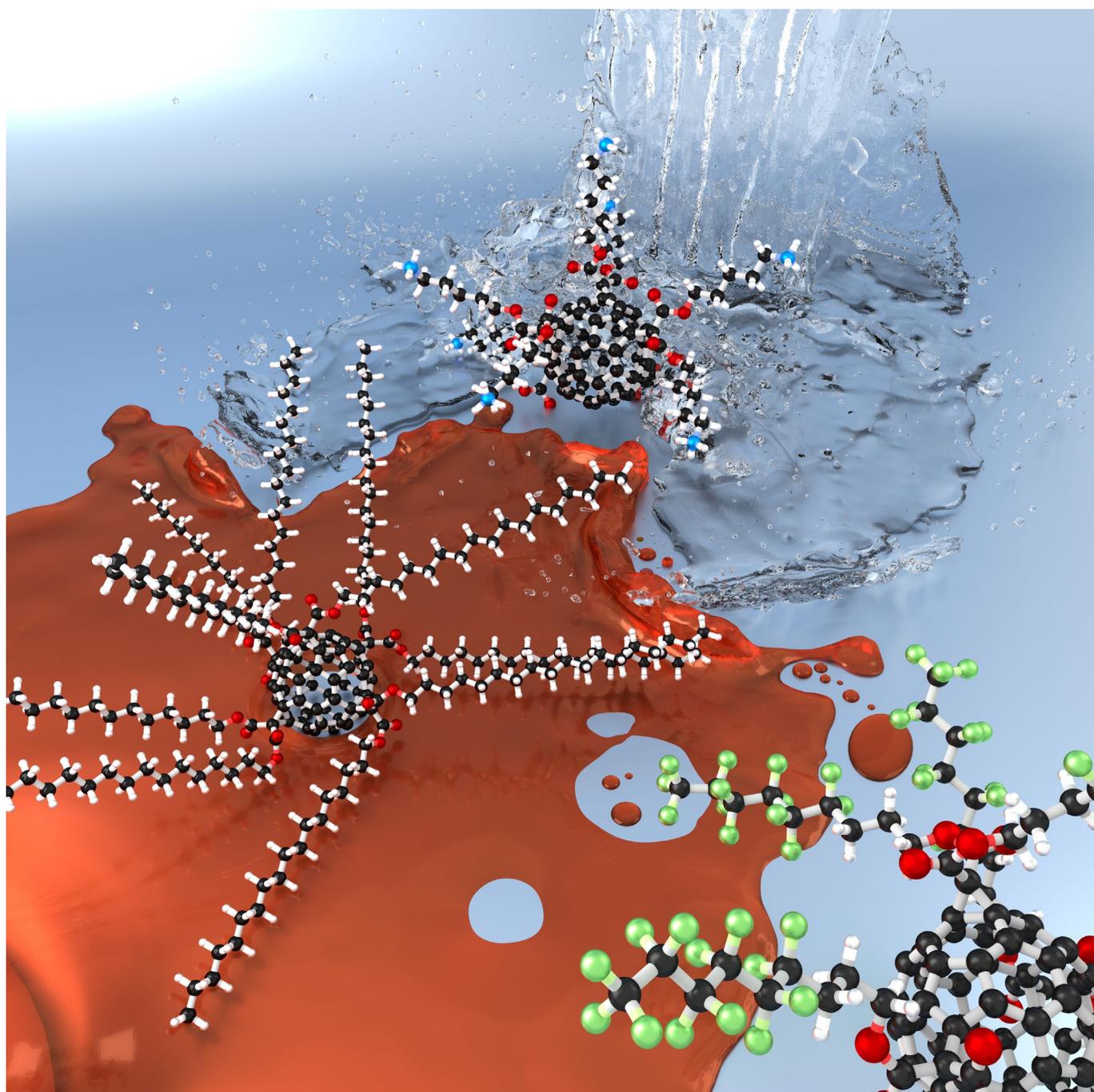
Abstract: Herein, the synthesis of fullerene derivatives with adjustable polarities and lyotropic aggregation properties is reported. The polarity range spans from superhydrophobic to hydrophilic, while simultaneously providing a further reactive position with a view to graft them onto other materials. The synthetic strategy relies on a selective protection with an isoxazoline moiety. The remaining octahedral positions were further functionalized with the desired groups to tune their solubility, yielding mixed [5:1] hexakisadducts. The sub-

sequent deprotection by clean photolytic reaction led to fullerene pentakisadducts with an incomplete octahedral addition pattern, which are useful forerunners for the synthesis of building blocks. Their hydrophobic/hydrophilic behavior has been characterized both in solution and surface through octanol/water partition coefficients (log P) and contact angle measurements. Furthermore, these derivatives can form supramolecular constructions which have been studied by dynamic light scattering (DLS) and cryo-TEM.

Introduction

Carbon exists in two natural allotropes, diamond and graphite. Other identified synthetic carbon allotropes include the 0D fullerenes which were observed for the first time by Kroto et al. in 1985, and the one-dimensional carbon nanotubes (CNT) which were first synthesized in 1991. The two-dimensional carbon allotrope, graphene, was isolated in 2004 and won the Nobel Prize in Physics in 2010.[1] Over three decades of research in fullerene chemistry have been dedicated to produce stable and well-characterized derivatives, which have been applied in a wide number of fields due to their outstanding properties.[2] However, fundamental research is still required to take real advantage of their properties on an industrial level. To increase synthetic carbon allotropes dispersability in solvents, raise their processability, reach stable exfoliation and facilitate their covalent functionalization onto other materials remains a challenge.[3] Furthermore, the nanomorphology-efficiency relationship has been already demonstrated for several devices.[4] The ability to control the interplay between chemical composition, solubility, and compatibility is a very useful tool to trigger the final properties and performance.

The development of a straightforward methodology for the selective functionalization of fullerenes enables the tuning of the solubility and provides additional reactive positions which

allow for directly grafting them onto other allotropes. In this way, the fullerenes with tailored solubility would serve as vector scaffolds to induce their solubility behavior to the materials where they are incorporated.

The solubility of nanocarbons is of paramount importance for their practical application, thus their water solubility and dispersability in other solvents have been previously targeted using various approaches, including the use of surfactants,[5] by oxidation (graphene oxide, GO),[6] by twisting molecular angles to avoid π–π stacking,[7] by supramolecular interactions with other molecules such as perylene bisimide[8] or melamine,[9] and through covalent functionalization.[10] Additionally, some amphiphilic fullerenes have been prepared.[11] Particularly for fullerenes, most of these systems are either mono- or hexa-adducts with no further reactive groups, and cannot be used as nanobuilding blocks for the controlled preparation of hybrid materials. To overcome that, we herein report the synthesis of different fullerene derivatives, ranging from superhydrophobic to hydrophilic, by using a synthetic strategy based on the selective protection of one fullerene's octahedral position with an isoxazolino moiety.[12] After systematically modifying their solubility as demanded, a mild photolytic deprotection and functionalization with a proper anchoring group can be carried out. The fullerene nanobuilding blocks with tuned behaviors can be further used in a lego-like approach to combine them with other materials.[13]

[a] Dr. M. E. Pérez-Ojeda, I. Wabra, Prof. Dr. A. Hirsch
Department of Chemistry and Pharmacy
Friedrich-Alexander-University Erlangen-Nuremberg
Nikolaus-Fiebiger-Straße 10
91058 Erlangen (Germany)
E-mail: andreas.hirsch@fau.de

[b] Dr. C. Böttcher
Forschungszentrum für Elektronenmikroskopie
Institut für Chemie und Biochemie
Freie Universität Berlin
Fabeckstr. 36a
14195 Berlin (Germany)
E-mail: christoph.boettcher@fzem.fu-berlin.de

Results and Discussion

For the selective synthesis of the fullerene derivatives our previously described methodology was used.[14] The three-step sequence starts with the mono-protection using an isoxazoline moiety as the protective group (Scheme 1, compound **1**), followed by a five-fold cyclopropanation with bis-malonates bearing different polarities and functional groups (**a**–**i**) via the Bingel–Hirsch reaction (Scheme 1, compound **2**) in the presence of CBr$_4$ and DBU as a non-nucleophilic base for the in situ generation of the α-bromomalonate,[15] and finally deprotection (Scheme 1, compound **3**). This very facile divergent strategy allowed us to access mixed [5:1] hexakisadducts **2a**–**i** through functionalization with hydrophobic (**2a**–**e**, **2g**-$_{tBu}$ and **2h**-$_{BOC}$), hydrophilic (**2f**–**h**), and polyfluorinated (**2i**) substituents in moderate yields (22–48%) (see Table 1).

Scheme 1. Synthesis of fullerene derivatives with different solubilities: hydrophobic (red), hydrophilic (blue) and super-hydrophobic (green) prepared via selective protection (**1**), Bingel–Hirsch reaction on the remaining positions with the corresponding bismalotanes (**2 a–i**) and photolytic deprotection to yield the functional pentakisadducts (**3 a–i**).

Table 1. Isolated yields for the synthesis of fullerene derivatives.		
	2 [yield %] [5:1] Bingel–Hirsch	**3** [yield %] [5:0] deprotection
a	38	63
b	48	63
c	26	72
d	35	87
e	27	67
f	45	55
g-tBu	22	59
h-Boc	27	96
i	non-isolated pure	51

Figure 1. ^{13}C NMR spectrum of compound **3 c** showing an expansion of the fullerene C-sp^2 region which confirms a successful deprotection and generation of a [5:0] pentakisadduct.

These yields are reasonable for a fivefold cyclopropanation proceeding selectively at the equatorial sites and moreover are comparable to other multiple-fold Bingel–Hirsch reactions reported previously.[14] After photolytic cleavage of the isoxazoline by retro-cycloaddition in presence of maleic anhydride, the desired C_{2v}-symmetrical pentakisadducts (**3 a–i**), with an incomplete octahedral addition pattern, were obtained in very good yields (51–96 %) (Table 1).

The structure of all [5:1] and [5:0] fullerenes was unambiguously confirmed by spectroscopic techniques, including multinuclear NMR and UV/Vis spectroscopy, as well as mass spectrometry (ESI-MS) and MALDI-TOF (for more details see Experimental Section and Supporting Information).

All mixed [5:1] hexakisadducts **2 a–i** showed complex ^{13}C NMR spectra with a high number of signals ($\approx$24) in the region between 150–138 ppm, corresponding to the 48 sp^2 carbon atoms of the fullerene core. This is due to the asymmetric substitution caused by the isoxazolino ring. In contrast, the deprotected pentakisadducts **3 a–i** showed, as expected, much simpler spectra. In this case only 13 resonances (12 with double intensity) are observed which can be assigned to the 50 sp^2 carbon atoms reflecting the C_{2v} symmetrical [5:0] pat-

tern and thus confirming the successful deprotection. The ^{13}C spectrum of compound **3 c** is shown in Figure 1 as an illustrative example. These results are in agreement with our previous work.[11b, 14, 16]

Additionally, the successful isoxazolino deprotection to yield the desired pentakisadducts **3 a–i** was nicely corroborated by the UV/Vis spectra showing distinct bands at $\lambda = 211$, 244, and 282 nm, as well as a very weak shoulder at $\lambda = 316$ nm (Figure 2). The fingerprint area (400–600 nm) in the visible region of the spectrum corresponds well to the characteristic pattern for pentakisadducts.[17]

Functionalization of the remaining position can be carried out under normal Bingel–Hirsch conditions, as we have previously described,[13] with functional malonates bearing anchoring groups as, for instance, alkyne groups or azides that can

Figure 2. UV/Vis spectra of compounds **3a–i** in different solvents depending on their solubility, reflecting the corresponding pattern for fivefold addition. A) compounds **3b**, **3c**, **3f**, **3g**$_{-tBu}$ and **3h**$_{-BOC}$ in octanol and expansion of the fingerprint area. B) compounds **3f–h** in phosphate buffer at pH 7.0 and C) compound **3i** in Freon 113.

be further used in click reactions to bind other building blocks with the soluble fullerenes.

Finally, the protecting groups in derivatives **3g**-t_{Bu} and **3h**-$_{BOC}$ were cleaved by treatment with 1:1 trifluoroacetic acid (TFA):toluene solution. The solubility of the corresponding fullerenes **3g** and **3h** was studied at three different pH-values in phosphate buffer (pH 4.4, 7.0, and 9.0) (see Supporting Information Figure S50 for further details). As expected, fullerene **3g** bearing ionizable carboxylic acids was soluble only at pH 9.0, whereas the derivative **3h** with the ionizable amines was only soluble at pH 4.4.

The hydrophobic/hydrophilic behavior and self-assembly properties for all the pentakisadducts **3a–i** were studied both in solution and on a solid surface. Their behavior in solution has been characterized by the octanol/water partition coefficients (log P), providing relevant information with regard to their possible fate and bio-accumulation for potential application in biomedicine. Contact angle measurements were used for the surface deposition characterization.

Contact angle measurements

Contact angle measurements were conducted on films prepared from the different fullerenes to study the influence of fullerene functionalization on the surface wettability. The contact angle of a surface is, among other factors, governed by the chemical composition, concretely by the hydrophilicity of its functional groups. Thus, in case of films with increasing hydrophilicity, the angle between the water droplet and the surface decreases as a result of a better hydration of interfacial groups and better surface wetting. Besides the polarity and composition of a surface, the contact angle also depends on the physical architecture: the surface micro-nanostructure. The

influence of hierarchical surface patterns on the wettability has been well established, and their effect translates into a considerable increase/decrease of the contact angle. This lotus leaf effect, has been widely applied in materials science to obtain superhydrophobic and self-cleaning surfaces.[18] Asanuma and co-workers described the influence of fullerene supramolecular polymorphism self-organization on the contact angle, reaching superhydrophobic values >150° for compounds bearing aliphatic chains that exhibit 103° when the film was spin-cast.[19] To minimize possible contributions from this effect, to avoid self-organization within the surface, and to examine exclusively the chemical contribution, fullerenes **3a–i** (5 mg mL^{-1} solution) were spin-coated on a glass wafer at 2500 rpm. The angles measured by the sessile drop (3 µL) technique are summarized in Table 2.

Facile chemical functionalization makes it possible to systematically modulate the fullerene behavior from hydrophobic angles close to 120° (similar to Teflon[20]) corresponding to perfluorinated derivative **3i**, to 50° for the hydrophilic **3h** and **3f** along the whole interval. However, an important drawback of this technique is that the water-soluble fullerenes **3f–h** get dissolved within the measurement time. Therefore, these values should only be qualitatively considered, and they are

Table 2. Static water contact angle ± standard deviation (deg.) of fullerene pentakisadducts **3a–i**.

i	c	d	b	a	h$_{-BOC}$	g$_{-tBu}$	e	g	h	f
118.7	112.6	111.4	106.3	89.0	92.6	87.6	74.9	75.2	55.7	47.1
±9.5	±2.3	±3.1	±2.8	±2.4	±1.0	±2.2	±3.3	±1.2	±1.0	±9.9

preferably characterized by the octanol/water partition coefficient. Despite that, we also carried out a pH dependent experiment. As expected, only the films containing ionizable fullerenes **3g,h** showed pH dependence of the contact angle.

To further clarify the correlation between the polarity of the individual functional group on the fullerene and the surface wettability, the results are rationalized by means of Hansch parameter π (also called the substituent constant), which describes the contribution of a substituent to the lipophilicity of a compound.[21] Contact angles were plotted as a function of available π-values obtained from the literature (Figure 3).[21,22] As expected, the more polar groups (with negative π-values) exhibit the lower contact angles, whereas the more hydrophobic substituents presented higher contact angle values. Pristine C_{60} has been also included as a reference considering $\pi = 0$ (no substituents) and contact angle of 91.5°.[23]
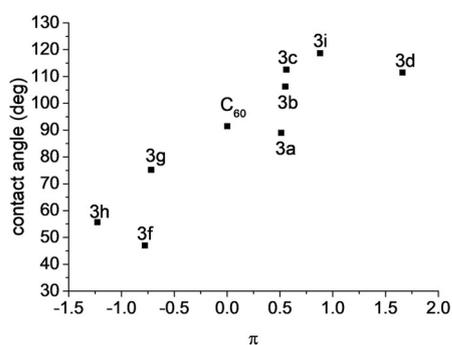
Figure 3. Experimental contact angle value as a function of the Hansch parameter π reflecting the expected tendency with the increase of polarity.

To evaluate the concentration influence on the contact angle, we also studied the contact angle on spin-cast films, prepared from more concentrated solutions that would lead to thicker films (20 mg mL^{-1}) under the same speed and acceleration conditions (see Supporting Information Figure S51 for additional details). Excluding the water-soluble fullerenes **3f–h**, particularly interesting is compound **3c** bearing the longer alkyl chain (C_{18}) that shows a remarkable increase in the contact angle from 112.6 ± 2.3° to 140.6 ± 6.3°, proximate to the superhydrophobic value (150°) This result could be interesting for engineering self-cleaning surfaces. This enhancement is presumably due to self-assembly/interdigitation (as will be further explained) of the stearyl chains that may induce some kind of the aforementioned surface structuring.

Estimating octanol-water partition coefficients

The octanol/water partition coefficient P or K_{ow} is defined by Equation (1) where c_o is the fullerene concentration in octanol and c_w is the fullerene concentration in water phase. This parameter displays a very useful method to establish the relative lipophilicity of a compound since it is a measure of the difference in solubility in two phases. In our study, this ratio was evaluated using the stirring flask method and 48 h equilibration time. The remaining concentrations in each phase after

Table 3. Octanol/water partitioning values.

	$\log P$	$\log P$ (dried)	$\Delta\log P$
C_{60}[24]	6.54		
3b	1.94 ± 0.15	2.24 ± 0.76	0.30
3c	0.46 ± 0.01	1.24	0.78
3f	0.62 ± 0.07	1.07	0.45
3g$_{-tBu}$	1.06 ± 0.001	0.94 ± 0.13	−0.12
3h$_{-Boc}$	0.63 ± 0.01	0.65	0.02
3g (pH9.0)	−0.32 ± 0.10	−0.62	0.30
3h (pH4.4)	−1.06 ± 0.03	−1.01	0.05

equilibration were assessed by UV/Vis absorption and the results are summarized in Table 3. The partition coefficient for C_{60} has been included from literature[24] as a reference value.

$$\log P = \log K_{ow} = \log \frac{c_o}{c_w} \tag{1}$$

As intended, chemical functionalization dramatically influences the fullerene distribution among octanol and water and modulates their behavior from strongly hydrophobic fullerenes, with positive log P values (Table 3, **3b,c**) to hydrophilic ones with negative values (Table 3, **3g,h**). All neutral fullerenes, including the water-soluble derivative **3f**, showed a positive log P value and only the fullerenes bearing ionizable groups showed a higher tendency towards water phase (see Supporting Information Figure S49 for further details). The negative values obtained for these hydrophilic fullerenes **3g,h** are in good agreement with other water soluble fullerene trisadducts previously described.[25]

Surprisingly, derivative **3c** was not the most hydrophobic one and displayed a lower log P value than would have been expected for a stearic-functionalized system. Besides, unlike other compounds, the octanol phase containing **3c** was not transparent but rather opaque, like an emulsion, suggesting water encapsulation (see Supporting Information Figure S48 for further details). To assess this possibility a simple drying process with $MgSO_4$ anhydrous was carried out. The emulsion turned into a clear solution and the $MgSO_4$ formed large clumps as a result of water adsorption. The concentrations and log P were reevaluated (Table 3) after this drying process. The difference between the initial log P value and the one after drying gives an indirect evidence of the systems with higher tendency to water encapsulation; being **3c**, as suspected, the more occluding one. With the intention of unraveling the eventual organization of these compounds in solution we carried out further studies on its supramolecular morphology.

Supramolecular self-assembly

Increasing attention has been devoted to supramolecular arrangement of fullerenes since it has been demonstrated that their physicochemical and electronic properties can be regulated based on the interaction among self-organized structures.[26] Most examples are based on amphiphilic fullerenes which display different self-assembly driven by hydrophobic/hydrophilic interactions with the solvent.[27] Also, some non-amphiphilic

fullerenes derivatives bearing mesogenic groups[28] and lipids[26,29] as a source of liquid crystalline organization have been studied. The thermotropic behavior of these so called lipo-fullerenes has been investigated. Likewise, differential scanning calorimetry (DSC) of pentakisadduct **3c** shows two endotherm transitions (see Supporting Information Figures S52 and S53) similar to the ones described in the literature for the homologous hexakisadduct.[29c] This has been attributed to different structural arrangements based on interdigitations of the lipidic addends. However, to the best of our knowledge, this comportment has only been addressed in the solid state, and this is the first example of non-amphiphilic fullerene displaying self-organization in solution.

To further confirm the self-assembly of **3c** in the octanol/water system, we evaluated the hydrodynamic diameter by means of dynamic light scattering (DLS). Figure 4A shows the number-weighted mean hydrodynamic diameter (D_h), calculated from a cumulate fit of the autocorrelation function (for comparison with the intensity-weighted distribution see Figure 4B). As expected, the size distribution centered at 1690 ± 123 nm is far away from the fullerene nominal size. The latter characteristic lengths derived from diffraction patterns for the analogous hexakisadduct,[29c] is calculated to be 6.1 ± 0.1 nm on its total extended conformation and $1.35 \pm 0.2/ 4.80 \pm 0.1$ nm for the interdigitated state, thus confirming the aggregation process. Moreover, the distribution was homogeneous and stable over time.

A dilution experiment was also carried out by adding increasing volumes of octanol (Figure 4B). The size distribution was found to be dependent on fullerene concentration up to 1×10^{-5} M. For this concentration, an asymptote is reached at a stable value of 375 ± 45 nm. We hypothesize the formation of smaller aggregates, such as vesicle-like structures capable of water entrapping, which can further collapse at concentrations $> 1 \times 10^{-5}$ M to create larger structures. Additionally, we studied the system in a different solvent to elucidate the process. THF was the solvent of choice for the titration experiment with successive water addition (Figure 4C). No aggregates were observed for the initial **3c** solution ($c = 2 \times 10^{-4}$ M) in THF. Promptly after water addition, aggregates of around 300 nm are formed. This definite diameter is similar to the one observed in the octanol dilution experiment (Figure 4B). Successive water additions gave rise to larger structures, which are in agreement with the previously observed diameters in octanol. The conjoint results suggest again the vesicle/liposome-like formation which entraps water inside. Additionally, these results indicate a further aggregation at high water concentration in the media, as it is the case for the experimental set-up in the biphasic stirring flask method. Similar vesicle structures, with membranes consisting of an interdigitated bilayer of the fullerenes, have been previously described in the literature for amphiphilic compounds,[30] but have never been observed for non-amphiphilic fullerenes before.

The self-assembly morphology was further evidenced by cryo-transmission electron microscopy (cryo-TEM) and tomography (cryo-ET). Figure 5A depicts a stereo image pair (8°-tilt) of a volume reconstruction obtained from a tilt series ($\pm 65°$ with 2° tilt-increment) recorded of compound **3c** in the octanol phase from the partition coefficient experiment. The 3D volume shows a population of vesicle-like assemblies in the 50–200 nm diameter range, which is reasonably in agreement with the results observed by DLS. For clarity, the contrast in
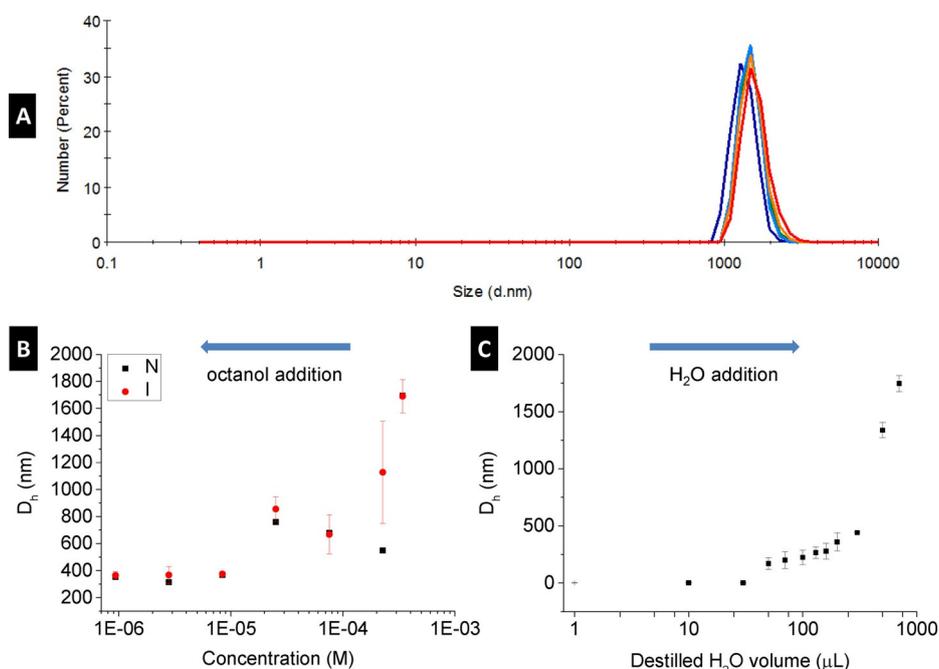
Figure 4. DLS A) Size distribution by number of fullerene **3c** in octanol $c = 2 \times 10^{-4}$ M (after partition coefficient experiment). Six consecutive measurements are included to show its consistence. B) Hydrodynamic diameter (D_h) expressed by number (N) and intensity (I) as a function of fullerene concentration in octanol (dilution experiment). C) DLS titration in THF. Hydrodynamic diameter (N) of fullerene **3c** in THF as a function of distilled water content.
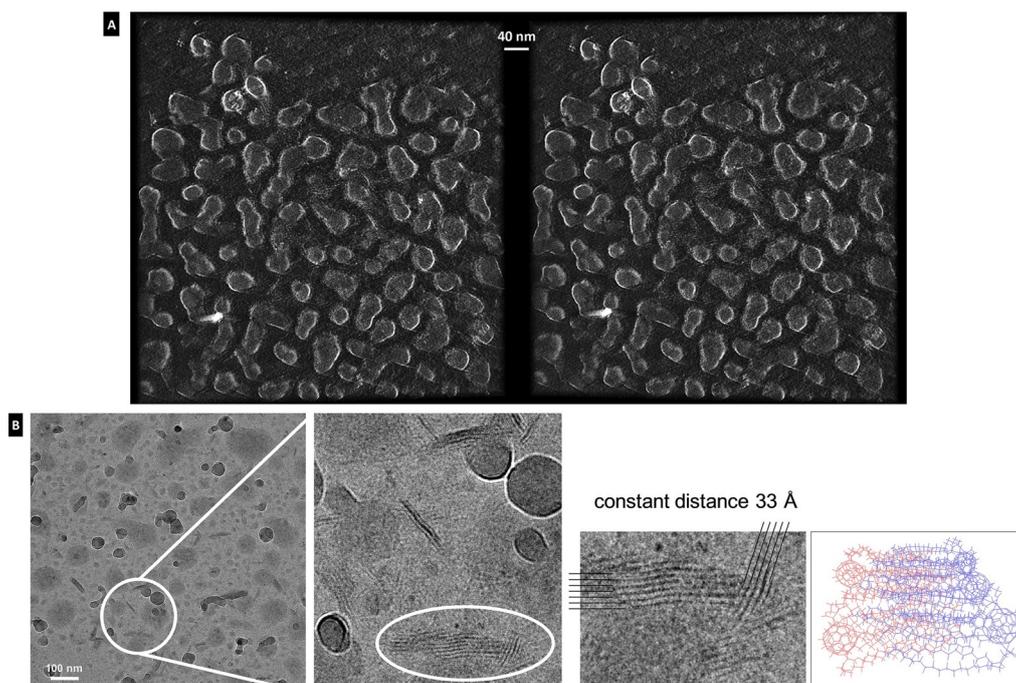
Figure 5. A) Stereo image pair (8°-tilt) of a volume stack of images reconstructed from a cryo-electron tomographic series (±65° in 2°-tilt increment) of the self-assembled vesicles and lamellar structures of **3c** in octanol/water system. The data are depicted in the Voltex modus of AMIRA software. Densities are inverted for clarity. B) Conventional cryo-TEM images of the self-assembled vesicles and lamellar structures of **3c** in octanol/water system with constant lattice distant of 33 Å and explicative cartoon showing the plausible interdigitated lamellar structure.

the image is inverted. The vesicle membrane (white) is very prominent and its thickness can be determined to amount to 3.0 ± 0.5 nm. Such high contrast, accurate spatial definiteness and dimension can only be attributed to a membrane-like assembly of the fullerene compound **3c** in an interdigitated arrangement of the stearyl-side-chains. Moreover, conventional cryo-TEM images also clearly indicate that the interior of the vesicles is of higher contrast compared to the exterior volume. Due to the differences in the density between octanol and water (ρ (octanol) = 0.817 g cm^{-3} vs. ρ (water) = 1 g cm^{-3}) we suggest that the fullerene vesicles enclose a water volume. Occasionally, elongated aggregates with striated profiles in lamellar-like structures with a constant repetitive distance of 3.3 ± 0.2 nm (marked in Figure 5B) are observed. The repetitive distance is of the same order as the individual membrane, and obviously reflects an alternate state of aggregation, which does not involve the encapsulation of larger water droplets. This kind of assembly behavior has also previously been observed in amphiphilic fullerene ultrastructures.[27a]

Despite that the vesicle formation is empirically proven by cryo-TEM tomography, their structural organization is still not clear. There are different factors (polar ester groups resulting from the Bingel–Hirsch reaction, the non-polar "naked" fullerene sixth position, long alkyl chain interdigitation, and possible umpolung effect mediated by the octanol) that could be contributing to different fullerene's orientation, but none of them looks sharply prevailing to conclude the fullerene's orientation within the vesicle. However, due to the fact that derivative **3c** is not amphiphilic and that interdigitation is proven in the solid state, we hypothesize that the driving force for vesicle

formation might be attributed to the interdigitation of hydrophobic stearyl chains in the presence of water in the biphasic forced environment.

Conclusions

Fullerene derivatives with different solubilities have been prepared by facile selective chemical functionalization. These derivatives have an additional position that can be functionalized with anchoring groups to further use them as nanobuilding blocks. Their solubility behavior has been systematically characterized both in solution and on surfaces through octanol/water partition coefficients (log *P*) and contact angle measurements, respectively. The ability to tune their performance through the whole interval ranging from hydrophobic contact angles similar to Teflon-like structures (approximately 120°) to hydrophilic angles of 50° degrees has been demonstrated. The log *P* values could also be modulated, ranging from +2.24 to −1.01. These derivatives are very promising for interfacial engineering as vectors to induce their solubility character to other allotropes and materials.

Interestingly, the fullerene **3c**, bearing ten long alkyl chains, forms hierarchical superstructure assemblies, as has been evidenced by DLS and cryo-TEM measurements. This is, to our knowledge, the first example of self-assembly in solution for non-amphiphilic fullerenes, which is probably driven by the interdigitation of the stearic chains in the forced octanol/water biphasic environment.

Our construction methodology is a powerful tool to modulate the properties through chemical functionalization, in order

to improve solubility and blending. The results of the present study will facilitate the application of these materials for industrial and technological uses by providing a catalogue of à la carte fullerene derivatives. In addition, these results provide compelling information towards the better understanding of non-amphiphilic fullerenes hierarchical assembly which is of great interest in nanoscience.

Experimental Section

Materials and methods

All chemicals were purchased from chemical suppliers and were used as received. C_{60} (99.0%) was purchased from IoLiTec nanomaterials and the sodium phosphate buffer solutions from Alfa Aesar. Reactions were monitored by thin layer chromatography (TLC) on silica60F254 0.2 mm on aluminum foil (Merck). Silica gel 60 M (230–400 mesh ASTM, 0.04–0.063 mm) from Marcherey-Nagel& Co. KG was used for column chromatography.

UV/Vis-NIR Spectroscopy: Spectra were recorded on a Shimadzu UV-1800 PC, scanning spectrophotometer. The absorption maxima λ_{max} are given in nm, and shoulders are denoted as sh. The spectra were measured in the indicated solvents in quartz cuvettes (edge length = 1 cm) at room temperature.

IR Spectroscopy: Spectra were recorded on a Bruker Tensor 27, Pike MIRacleTM ATR, Pike Technologies. Absorptions are given in wavenumbers $\tilde{v}$ (cm^{-1}).

NMR Spectroscopy: NMR spectra were recorded on, Bruker Avance 400 (400 MHz), Jeol EX 400 (400 MHz), and Jeol EX500 (500 MHz) spectrometers. Chemical shifts are given in ppm and are referenced to residual solvent signals and reported relative to external $SiMe_4$.

Mass spectrometry: Spectra were recorded on Bruker microTOF II focus (Bruker Daltonik GmbH) and Shimadzu Axima Confidence maXis 4G instruments (Nitrogen UV laser, 50 Hz, 337 nm). MALDI-TOF HRMS were recorded on a Bruker UltrafleXtreme TOF/TOF and trans-2-[3-(4-tert-butylphenyl)-2-methyl-propenylidene]malonitrile (DCTB) and 2,5-dihydroxy-benzoic acid (DHB) were used as matrices. ESI mass spectra were obtained on Bruker microTOF II focus ESI-TOF spectrometer. The APPI mass spectra were recorded on Bruker maXis 4G TOF-mass spectrometer.

Contact angle measurements: Spin Coater WS-650-23 NPP/lite from Laurell Technologies was employed. Two series of films were prepared at 5 mg mL^{-1} and 20 mg mL^{-1}, respectively. The solutions (in dichloromethane, distilled water or Freon 113) were spin-coated on glass wafers at 2500 rpm with acceleration 500 during 10 s.

Static contact angle measurements were performed by using a contact angle goniometer (KSV Theta goniometer), with the sessile drop method. Deionized water droplets of 3 μL were placed on the films and a coupled device camera was used to capture the images of the water droplets for the determination of the contact angle. The measurements were performed at both sides of the droplet. Three to five droplets were analyzed for each composition.

Cryogenic transmission electron microscopy (cryo-TEM): Cryo-sample preparation: The cryo preparation was accomplished by applying octanol droplets from the biphasic octanol/water sample solution ($c = 2 \times 10^{-4}$ M) to 200 mesh holey carbon film gold grids (R1/4 batch of Quantifoil Micro Tools GmbH, Jena, Germany), which had been previously covered with a Graphene Oxide layer (provided by Dr. P. Feicht, FU Berlin). An ultra-thin layer of the sample solution was prepared by removing the supernatant fluid with a filter

paper. The samples were immediately vitrified by propelling the grids into liquid nitrogen (instead of liquid ethane commonly used to avoid unwanted dissolution of octanol). The vitrified grids were stabilized by a copper autogrid and fixed by a spring clamp under liquid nitrogen. The vitrified samples were transferred under liquid nitrogen into a Talos Arctica transmission electron microscope (ThermoFisher Scientific Inc., Waltham (MA), USA) using the microscope's autoloader protocol. Imaging was performed using the microscope's low-dose protocol at a primary magnification of 28 000x and an acceleration voltage of 200 kV. Image were recorded by a Falcon 3CE direct electron detector (64 aligned frames) at full size (4k). The defocus was chosen to be 4.90 μM in all cases to create sufficient phase contrast.

A control experiment was performed on pure octanol/water to exclude the possibility of artefact preparation by using the liquid nitrogen freezing protocol and confirming that all reported supramolecular structures can be unambiguously attributed to the fullerene assemblies (See Supporting Information Figure S54). The blank octanol/water sample also displayed ordered areas with a very consistent layer lines of 26 Å, which exactly correspond to the value of an octanol bilayer arrangement (expected in a polar aqueous environment) considering the length of the molecule according to the crystal data ($2 \times \approx 13$ Å) but is different from the values measured in the presence of fullerene compounds (33 Å).

To explore the three-dimensional organization of the supramolecular fullerene assembly structures in more detail we recorded tomographic image series with the Talos Arctica Kryo-TEM using the FEI Tomography package ($\pm 65°$ in $2°$- tilt angle increments). Alignment and reconstruction was performed in the context of ThermoFisher Inspect 3D software, visualization with ThermoFisher AMIRA 6.0.

Dynamic light scattering: The measurements were carried out in a Zetasizer Nano series ZEN3600 (Malvern Instruments) provided with a red laser (633 nm). $173°$ angle (NIBS, "noninvasive back scatter") was used. Three consecutive measurements were performed after an equilibration time of 60 s.

Octanol/water partition coefficient: The stirring flask method was used with an initial fullerene concentration of 10^{-4} M in octanol, which was previously saturated with water. The water phase was buffered at pH 7 for all neutral fullerenes (**3a–f**) using a sodium phosphate buffer (0.5 M). Even though log P is described as the partition equilibrium for neutral species, the log P of fullerenes **3g** and **3h** were evaluated under their ionized form due to solubility problems. Phosphate buffered water at pH 9.0 (0.5 M) for **3g** and at pH 4.4 (0.2 M) for **3h** were used. For the biphasic solutions, 2 mL of each phase were placed in a glass vial and were stirred at high speed at room temperature. Since the equilibration time may play an important role in slow distribution equilibriums, it was fixed at 48 h for all the samples. The concentration in each phase was evaluated via UV/Vis measurements. For the log P dried, anhydrous $MgSO_4$ was added to the octanol phase to remove possible encapsulated water. The phase was filtered to remove the $MgSO_4$ and re-evaluation of the fullerene concentration in octanol was conducted. All experiments were carried out in duplicate (see Supporting Information). Fullerenes **3a**, **3d** and **3i** were not evaluated due to their low solubility in both octanol and water.

Differential scanning calorimetry: The thermotropic behavior of fullerene **3c** was investigated by DSC with a NETZSCH STA 409 C/CD thermal analysis system. The measurement was carried out in flowing helium for both heating and cooling cycles at a ramp rate of $1°C$ min^{-1}. It was also evaluated under a faster heating rate with a Mettler Toledo DSC821e and evaluated with Mettler Star SW 8.10 Thermal analysis software.

Synthetic procedures

Synthesis of precursor malonates: Malonates **a**, **b** and **d** are commercially available and were used as purchased. Malonates **c**,[31] **e**,[32] **f**,[33] **g-tBu**[34] and **i**[35] were prepared from malonyl dichloride and the corresponding alcohols following literature procedures. Malonate **h-BOC**[36] was prepared from malonic acid and *tert*-butyl 6-hydroxyhexylcarbamate with N,N′-dicyclohexylcarbodiimide (DCC) and 4-dimethylaminopyridine (DMAP).

Synthesis of isoxazolinofullerene precursor (1) The synthesis was performed according to the method previously described in the literature.[12]

General procedure for the synthesis of mixed [5:1] fullerene hexakisadducts (2a–i)

The Bingel–Hirsch reaction was carried out following the methodology previously described in our group.[13,14] Compound **1** (1 equiv.) was dissolved in dry toluene ($\approx 7 \times 10^{-4}$ M) together with CBr$_4$ (100 equiv.) and the corresponding malonate (12 equiv.). The solution was stirred for 1 h under exclusion of light and nitrogen atmosphere at room temperature. Subsequently, 1,8-diazabicyclo[5.4.0]undec-7-ene (DBU) (24 equiv.) dissolved in toluene (5–10 mL) was added over 30 min. and the reaction mixture was stirred until completion (monitored by TLC). The crude product was plug-filtered (SiO$_2$) and purified by column chromatography.

Compound 2a:[14] The synthesis was performed according to the general procedure with **1** (150 mg, 0.170 mmol) dissolved in dry toluene (250 mL) together with CBr$_4$ (5.65 g, 17 mmol) and diethyl malonate (285 µL, 1.170 mmol). After 1 h, DBU (0.5 mL 3.4 mmol) dissolved in toluene (10 mL) was added over 15 min, and the reaction mixture was stirred for additional 72 h. The crude product was plug-filtered (SiO$_2$; toluene/ethyl acetate 9:1) and purified by column chromatography (SiO$_2$; toluene/ ethyl acetate 95:5) to obtain fullerene **2a** (107 mg, 0.071 mmol, 38%) as a yellow-orange solid. R_f (toluene: ethyl acetate 9:1) = 0.45; ^{1}H NMR (400 MHz, CDCl$_3$, rt): δ = 7.87 (d, J = 9.1 Hz, 2H, H_{ortho}), 6.68 (d, J = 9.1 Hz, 2H, H_{meta}), 4.45–4.14 (m, 20H, CH_2), 2.97 (s, 6H, N(CH_3)$_2$), 1.43–1.24 ppm (m, 30H, CH_3); ^{13}C NMR (100.5 MHz, CDCl$_3$, rt): δ = 164.22, 164.15, 164.07, 163.86, 163.80, 163.77 (10C, CO), 154.78 (1C, C=N), 151.54 (1C, CN(CH$_3$)$_2$), 147.09, 146.98, 146.74, 146.53, 146.27, 146.18, 145.71, 145.63, 145.53, 144.30, 143.96, 143.46, 142.41, 142.01, 141.51, 141.43, 140.60, 139.89, 139.69, 139.41 (48 C, C$_{60}$-sp^2), 129.76 (2C, C_{ortho}), 116.75 (1C, C_{ipso}), 111.77 (2C, C_{meta}), 101.63 (1C, C$_{60}$-sp^3 C-O isox), 77.36 (1C, C$_{60}$-sp^3 C-C isox), 69.99, 69.32, 68.14, 67.53 (10C, C$_{60}$-sp^3), 63.13, 63.05, 62.59 (10 C, CH_2), 45.54, 45.39, 44.67, 41.92 (5C, COCCO), 40.16 (2C, N(CH$_3$)$_2$), 14.14, 14.08 ppm (10C, CH_3). MS (MALDI-TOF, dhb): m/z = 1511.3248 [M-isoxazoline]$^+$.

Compound 2b: The synthesis was performed according to general procedure with **1** (75 mg, 0.085 mmol) dissolved in dry toluene (125 mL) together with CBr$_4$ (2.825 g, 8.5 mmol) and dihexyl malonate (246 µL, 0.85 mmol). After 1 h, DBU (0.25 mL, 1.7 mmol) dissolved in toluene (5 mL) was added over 5 min and the reaction mixture was stirred for additional 4 days. The crude product was plug-filtered (SiO$_2$; toluene/ethyl acetate 9:1) and purified twice by column chromatography (SiO$_2$; toluene/CH$_2$Cl$_2$ 4:1, toluene/hexane 4:1 → toluene/hexane/ethyl acetate 20:5:0.06) to obtain fullerene **2b** (91 mg, 0.036 mmol, 48%) as a yellow viscous liquid. R_f (hexane/ethyl acetate 6:1): 0.57; ^{1}H NMR (400 MHz, CDCl$_3$, rt): δ = 7.87 (d, J = 9.0 Hz, 2H, H_{ortho}), 6.67 (d, J = 9.1 Hz, 2H, H_{meta}), 4.43–4.03 (m, 20H, OCH_2), 2.97 (s, 6H, N(CH_3)$_2$), 1.86–1.58 (m, 20H, OCH$_2$CH_2), 1.43–1.08 (m, 60H, CH_2), 0.98–0.73 ppm (m, 30H, CH_3); ^{13}C NMR (100.5 MHz, CDCl$_3$, rt): δ = 164.29, 164.24, 164.24, 164.13,

163.94, 163.85, 163.76 (10C, CO), 154.76 (1C, C=N), 151.51 (1C, CN(CH$_3$)$_2$), 147.06, 146.77, 146.48, 146.25, 146.19, 145.91, 145.70, 145.66, 145.56, 145.46, 144.26, 143.92, 143.48, 142.46, 142.04, 141.99, 141.49, 141.37, 140.64, 139.91, 139.76, 139.69, 139.63 (48C, C$_{60}$-sp^2), 129.75 (2C, C_{ortho}), 116.83 (1C, C_{ipso}), 111.81 (2C, C_{meta}), 101.68 (1C, C$_{60}$-sp^3 C-O isox), 77.36 (1C, C$_{60}$-sp^3 C-C isox), 70.07, 69.39, 68.22, 67.62, 67.24, 67.15, 63.37 (10C, C$_{60}$-sp^3 and 10C, OCH_2), 45.67, 45.55, 44.80, 42.06, 41.46 (5C, OCCCO), 40.15 (2C, N(CH$_3$)$_2$), 31.46, 31.43, 31.41, 31.40 (10C, CH_2), 28.49, 28.44 (10C, CH_2), 28.42, 25.60, 25.58, 25.54, 25.53, 25.50 (10C, CH_2), 22.62, 22.61, 22.58 (10C, CH_2), 14.09, 14.08, 14.06, 14.05 ppm (10C, CH_3); MS (MALDI-TOF, dctb): m/z = 2233 [M]$^+$, 2071 [M-isoxazoline]$^+$.

Compound 2c: The synthesis was performed according to general procedure with **1** (100 mg, 0.113 mmol) dissolved in dry toluene (165 mL) together with CBr$_4$ (3.758 g, 11.33 mmol) and distearyl malonate (826 mg, 1.356 mmol). After 45 min, DBU (405 µL, 2.71 mmol) dissolved in toluene (5 mL) was added over 10 min and the reaction mixture was stirred for additional 5 days. The crude product was plug-filtered (SiO$_2$; cyclohexane/CH$_2$Cl$_2$ 3:7) and purified twice by column chromatography (SiO$_2$; cyclohexane/CH$_2$Cl$_2$ 2:1→1.5:1) to obtain fullerene **2c** (112.4 mg, 0.029 mmol, 26%) as a waxy yellow solid. R_f (DCM:*c*-hexane, 1:1) = 0.26; ^{1}H NMR (400 MHz, CDCl$_3$, rt): δ = 7.87 (d, ^3J = 8.9 Hz, 2H, H_{ortho}), 6.68 (d, ^3J = 8.9 Hz, 2H, H_{meta}), 4.42–4.05 (m, 20H, OCH_2), 2.97 (s, 6H, N(CH_3)$_2$), 1.84–1.59 (m, 20H, OCH$_2$CH_2), 1.28 (bs, 320H, CH_2), 0.88 ppm (t, J = 6.8 Hz, 30H, CH_3); ^{13}C NMR (100.5 MHz, CDCl$_3$, rt): δ = 164.18, 164.12, 163.83, 163.74, 163.43 (10C, CO), 146.98, 146.70, 146.18, 146.16, 145.85, 145.65, 145.49, 145.35, 144.17, 143.85, 143.43, 142.37, 142.00, 141.89, 141.41, 141.29, 140.57, 139.83, 139.74, 139.63, 139.56, 138.23 (48C, C$_{60}$-sp^2), 132.62, 129.72 (2C, C_{ortho}), 115.56 (1C, C_{ipso}), 111.88 (2C, C_{meta}), 100.13 (1C, C$_{60}$-sp^3 C-O isox), 76.40 (1C, C$_{60}$-sp^3 C-C isox), 70.11, 70.09, 69.82, 69.42, 68.26, 67.66, 67.27, 67.19 (10C, C$_{60}$-sp^3 and 10C, OCH_2), 50.97, 45.71, 45.61, 44.85, 42.11 (5C, OCCCO), 40.26 (2C, N(CH$_3$)$_2$), 32.09 (10C, OCH$_2$CH_2), 29.90, 29.89, 29.86, 29.83, 29.79, 29.77, 29.73, 29.71, 29.62, 29.53, 29.46, 29.43, 29.41, 29.26, 28.65, 28.60, 28.58, 28.38, 26.05, 25.98, 25.75 (140C, CH_2), 22.85 (10C, CH_2), 14.26 ppm (10C, CH_3), signals for (1C, C=N), (1C, CN(CH$_3$)$_2$) were not observable; MS (MALDI-TOF, dctb): m/z = 3754.9584 [M-isoxazoline]$^+$, 3777.9016 [(M-isoxazoline)+Na]$^+$.

Compound 2d: The synthesis was performed according to general procedure with **1** (150 mg, 0.169 mmol) dissolved in dry toluene (250 mL) together with CBr$_4$ (5.622 g, 16.95 mmol) and dibenzyl malonate (636 µL, 2.54 mmol). After 45 min, DBU (763 µL, 5.1 mmol) dissolved in toluene (5 mL) was added over 10 min and the reaction mixture was stirred for additional 6 days. The crude product was plug-filtered (SiO$_2$; toluene → toluene/ethyl acetate 5:1) and purified by column chromatography (SiO$_2$; toluene/ethyl acetate 100:5) to obtain fullerene **2d** (135 mg, 0.058 mmol, 35%) as a yellowish-orange solid. R_f (toluene:hexane:ethyl acetate, 6:3.5:0.5) = 0.16; ^{1}H NMR (400 MHz, CDCl$_3$, rt): δ = 7.85 (d, J = 8.9 Hz, 2H, H_{ortho}), 7.50–6.96 (m, 50H, Ph-H), 6.68 (d, J = 8.9 Hz, 2H, H_{meta}), 5.28 (s), 5.26 (s), 5.24 (s), 5.24 (s), 5.19 (s), 5.18 (s), 5.15 (s), 5.10 (s) (20H, COCH_2Ph), 2.91 ppm (s, 6H, N(CH_3)$_2$); ^{13}C NMR (100.5 MHz, CDCl$_3$, rt): δ = 169.30, 164.03, 164.03, 163.89, 163.62, 163.58, 163.58, 163.55 (10C, CO), 146.98, 146.65, 146.42, 146.15, 146.05, 145.61, 145.59, 145.44, 145.42, 144.20, 143.87, 143.35, 141.99, 141.65, 141.09, 141.08, 140.24, 139.66, 139.35, 139.28, 139.18 (48C, C$_{60}$-sp^2), 134.74, 134.72, 134.71, 134.69, 134.67, 134.65, 134.59, 129.81, 129.20, 129.20, 129.12, 129.09, 129.08, 129.07, 129.05, 129.03, 128.98, 128.97, 128.95, 128.91, 128.89, 128.86, 128.81, 128.81, 128.79, 128.79, 128.77, 128.76, 128.73, 128.71, 128.65 (10C, C_{ipso}-Ph; 50C, CH-Ph and 2C, C_{ortho}), 111.81 (2C, C_{meta}),

101.52 (1C, C_{60}-sp^3 C-O isox), 77.36 (1C, C_{60}-sp^3 C-C isox), 69.76, 69.16, 68.83, 68.74, 68.71, 68.66, 68.34, 67.90, 67.37 (10C, COCH_2Ph and 10C, C_{60}-sp^3), 45.12, 44.99, 44.72 (5C, OCCCO), 40.13 ppm (2C, N(CH$_3$)$_2$), signals for (1C, C=N), (1C, C_{ipso}) and (1C, CN(CH$_3$)$_2$) were not observable; MS (MALDI-TOF, dctb): m/z = 2131.56 [M-isoxazo-line]$^+$, 2153.52 [(M-isoxazoline) + Na]$^+$.

Compound 2e: The synthesis was performed following a modified methodology.[32] Compound **1** (120 mg, 0.136 mmol) was dissolved in *ortho*-dichlorobenzene (o-DCB) (200 mL) together with CBr$_4$ (4.510 g, 13.6 mmol) and the corresponding malonate **e** (641 mg, 1.61 mmol). The solution was stirred for 30 min under exclusion of light and nitrogen atmosphere at room temperature. Subsequently, DBU (490 µL, 3.264 mmol) dissolved in o-DCB (5 mL) was added over 30 min and the reaction mixture was stirred for 3 days. The crude product was plug-filtered (SiO$_2$; toluene/ethyl acetate 1:1 → CHCl$_3$ 3% vol. pyridine) and purified twice by column chromatography (SiO$_2$, CHCl$_3$ 3% vol. pyridine) to obtain **2e** (104 mg, 0.036 mmol, 27%) as a brownish-orange solid. R_f (EtOAc 3% py) = 0.65; ^{1}H NMR (400 MHz, CDCl$_3$, rt): δ = 7.90 (d, J = 8.9 Hz, 2H, H_{ortho}), 7.22–6.98 (m, 20H, Ar-H), 6.95 (d, J = 8.9 Hz, 2H, H_{meta}), 6.80–6.53 (m, 20H, Ar-H), 4.65–4.06 (m, 20H, OCH_2), 3.01–2.67 ppm (m, 66H, N(CH_3)$_2$ and 20H, CH_2); ^{13}C NMR (100.5 MHz, CDCl$_3$, rt): δ = 167.73, 163.92, 163.57, 163.46 (10C, CO), 149.54, 149.46 (11C, CN(CH$_3$)$_2$), 146.83, 146.68, 146.19, 145.88, 145.69, 145.15, 142.28, 141.82, 141.29, 139.75, 139.68, 139.43 (48C, C_{60}-sp^2), 129.90, 129.80, 129.67, 129.57, 126.60, 125.36, 125.29, 125.18, 125.04, 122.75 (22C, CH-Ar), 113.91, 113.78, 113.36, 113.18, 112.90, 111.77 (22C, CH-Ar and 11C, C_{ipso}-Ar), 109.04, 70.07, 69.37, 68.82, 68.24, 67.86, 67.78, 67.72, 67.64, 67.49, 66.75, 64.04 (10C, COCH_2 and 10C, C_{60}-sp^3), 41.03, 40.93, 40.07, 38.27, 35.92, 34.27, 34.03, 33.85, 32.03, 31.06, 29.81 ppm (5C, OCCCO; 10C, CH$_2$ and 22C, N(CH$_3$)$_2$), signals for (1C, C=N), (1C, C_{60}-sp^3 C-O isox), 77.36 (1C, C_{60}-sp^3 C-C isox) were not identified; MS (MALDI-TOF, dctb): m/z = 2702.05 [M-isoxazoline]$^+$, 2726.96 [(M-isoxazoline) + Na]$^+$, 2864.29 [M]$^+$.

Compound 2f: The synthesis was performed according to general procedure with **1** (175 mg, 0.198 mmol, 1 equiv.) in dry toluene (270 mL) together with CBr$_4$ (6.559 g, 19.778 mmol, 100 equiv.) and bismalonate **f** (1.150 g, 2.373 mmol, 12 equiv.). The solution was stirred for 1 h under exclusion of light and nitrogen atmosphere at room temperature. Subsequently, DBU (723 mg, 710 µL, 14.747 mmol, 24 equiv.) was slowly added and the reaction mixture was stirred for 3 days. The crude product was plug-filtered (SiO$_2$; toluene/CH$_2$Cl$_2$/MeOH 4:5:1) and purified twice by column chromatography (SiO$_2$; CH$_2$Cl$_2$/ toluene/MeOH 100:60:12) to yield **2f** (147 mg, 0.155 mmol, 45%) as a dark yellow-orange oil. R_f (toluene:hexane 2:1) = 0.37; ^{1}H NMR (400 MHz, CDCl$_3$, rt): δ = 7.86–7.84 (d, J = 8.0 Hz, 2H, H_{ortho}), 6.68–6.66 (d, J = 8.0 Hz, 2H, H_{meta}), 4.46–4.31 (m, 20H, COOCH_2), 3.65–3.53 (m, 140H, OCH_2), 3.38–3.36 (s, 30H, OCH_3), 2.98 ppm (s, 6H, N(CH_3)$_2$); ^{13}C NMR (100.5 MHz, CDCl$_3$, rt): δ = 163.9, 163.6 (10C, CO), 151.7 (1C, CN(CH$_3$)$_2$), 149.8 (1C, C=N), 147.2, 147.0, 146.6, 145.7, 144.5, 144.1, 142.8, 142.0, 140.61, 140.2, 140.1, 139.7, 139.5 (48C, C_{60}-sp^2), 129.9 (2C, C_{ortho}), 116.8 (1C, C_{ipso}), 112.0 (2C, C_{meta}), 101.8 (1 C, C_{60}-sp^3 C-O isox), 76.6 (1 C, C_{60}-sp^3 C-C isox), 72.3, 70.9, 70.8, 68.9, 66.2 (80C, OCH_2 and 10C C_{60}-sp^3), 59.4 (10C, OCH_3), 45.7, 45.5, 42.0 (5C, OCCCO), 40.4 ppm (2C, N(CH$_3$)$_2$); MS (MALDI-TOF, dctb): m/z = 3156 [(M-isoxazoline) + Na]$^+$.

Compound 2g$_{-tBu}$:[14] The synthesis was performed according to modified procedure[32] with **1** (150 mg, 0.169 mmol) dissolved in o-DCB (250 mL) together with CBr$_4$ (5.622 g, 16.95 mmol) and malonate **g** (902 mg, 2.028 mmol). After 30 min, DBU (607 µL, 4.056 mmol) dissolved in o-DCB (5 mL) was added over 30 min and the reaction mixture was stirred for additional 8 days. The crude product was plug-filtered (SiO$_2$; toluene → toluene/ethyl acetate

4:1) and purified by column chromatography (SiO$_2$, toluene/ethyl acetate 9:1→85:15) to obtain **2g$_{-tBu}$** (117 mg, 0.038 mmol, 22%) as a yellowish-orange viscous oil. R_f (toluene:ethyl acetate 85:15) = 0.37; ^{1}H NMR (500 MHz, CDCl$_3$, rt): δ = 7.84 (d, J = 8.6 Hz, 2H, H_{ortho}), 6.67 (d, J = 8.6 Hz, 2H, H_{meta}), 4.41–3.99 (m, 20H, COOCH_2), 2.97 (s, 6H, N(CH$_3$)$_2$), 2.29–1.98 (m, 20H, CH_2COOtBu), 1.89–1.48 (m, 40H, CH_2), 1.43, 1.43, 1.41 (s, 90H, CH$_3$), 1.39–1.10 ppm (m, 20H, CH_2); ^{13}C NMR (126 MHz, CDCl$_3$, rt): δ = 173.07, 173.00, 172.97, 172.96, 172.92, 164.11, 163.96, 163.75, 163.66, (10C, COOtBu), 154.68 (1C, CN(CH$_3$)$_2$), 151.53 (1C, C=N), 147.02, 146.77, 146.68, 146.46, 146.24, 145.96, 145.72, 145.56, 145.37, 144.26, 143.91, 143.48, 142.36, 141.99, 141.85, 141.40, 141.24, 140.55, 139.84, 139.76, 139.63, 139.59 (48C, C_{60}-sp^2), 129.74 (2C, C_{ortho}), 116.78 (1C, C_{ipso})$_n$ 111.80 (2C, C_{meta})$_n$ 101.85 (1 C, C_{60}-sp^3 C-O isox)$_n$ 80.19, 80.17 (10C, C(CH$_3$)$_3$), 70.05, 70.03, 69.75, 69.37, 68.20, 67.61, (1 C, C_{60}-sp^3 C-C isox and 10C C_{60}-sp^3), 66.98, 66.89, 66.41 (10C, OCH_2), 45.57, 45.47, 44.72, 41.98 (5C, OCCCO), 40.17 (2C, N(CH$_3$)$_2$), 35.44, 35.40, 35.31 (10C, CH$_2$CO), 28.23 (10C, CH$_2$ and 30C, CH$_3$), 25.44, 25.37 (10C, CH$_2$), 24.75, 24.71, 24.61 ppm (10C, CH$_2$); MS (MALDI-TOF, dctb): m/z = 2956.23 [(M-isoxazoline) + Na]$^+$; HRMS (APPI): m/z calcd for $C_{184}H_{200}N_2O_{41}$: 2093.3615, found: 3093.3621 [M]$^+$.

Compound 2h$_{-BOC}$:[14] The synthesis was performed according to modified procedure[32] with **1** (150 mg, 0.169 mmol) dissolved in o-DCB (250 mL) together with CBr$_4$ (5.622 g, 16.95 mmol) and malonate **h** (1.015 g, 2.028 mmol). After 30 min, DBU (607 µL, 4.056 mmol) dissolved in o-DCB (5 mL) was added over 30 min and the reaction mixture was stirred for additional 7 days. The crude product was plug-filtered (SiO$_2$; toluene → toluene/ethyl acetate 4:1→1:1). Subsequently, it was purified by column chromatography (SiO$_2$, toluene → toluene/THF 3:1) to obtain **2h$_{-BOC}$** (158 mg, 0.046 mmol, 27%) as an orange viscous oil. R_f (toluene/ethyl acetate 1:1) = 0.44; ^{1}H NMR (400 MHz, CDCl$_3$, rt): 7.84 (d, J = 8.9 Hz, 2H; H_{ortho}), 6.64 (d, J = 8.9 Hz, 2H, H_{meta}), 5.00–4.67, 4.59 (bs, 10H, NH), 4.45–4.02 (m, 20H, OCH_2), 3.08 (m, 20H, CH_2NH), 2.95 (s, 6H, N(CH$_3$)$_2$), 2.06–1.45 (m, 40H, CH$_2$), 1.40 (s, 90H, CH$_3$), 1.36–1.24 ppm (m, 40H, CH$_2$); ^{13}C NMR (100.5 MHz, CDCl$_3$, rt): δ = 164.17, 164.10, 164.01, 163.87, 163.80, 163.72, 163.63 (10C; CO), 156.25 (10C, COOtBu), 154.59 (1C, C=N), 151.51 (1C, CN(CH$_3$)$_2$), 146.91, 146.72, 146.37, 146.11, 145.75, 145.57, 145.44, 145.28, 144.20, 143.84, 143.41, 142.35, 141.99, 141.89, 141.38, 141.32, 140.54, 139.83, 139.73, 139.61, 139.47 (48C; C_{60}-sp^2), 129.66 (2C, CH-Ar), 116.59 (1C, C_{ipso}), 111.70 (2C, CH-Ar), 101.53 (1C, C_{60}-sp^3 C-O isox), 79.12, 78.99 (10C, C(CH$_3$)$_3$), 69.97, 69.68 (1C, C_{60}-sp^3 C-C isox), 69.33, 68.13, 67.51, 66.99, 66.58 (10C, C_{60}-sp^3), 62.63 (10C, OCH_2), 45.61, 45.53, 44.73, 42.01 (5C, OCCCO), 40.50, 40.38 (10C, CH$_2$NH), 40.09 (2C, N(CH$_3$)$_2$), 32.59, 30.07, 29.97 (20C, CH$_2$), 28.46, 28.43, 28.34 (30C, CH$_3$), 26.40, 25.60, 25.56, 25.29 ppm (20C, CH$_2$); MS (MALDI-TOF, dctb): m/z = 3223.09 [M-isoxazoline]$^+$, 3147.06 [(M-isoxazoline) + Na]$^+$; HRMS (APPI): m/z calcd for $C_{194}H_{231}N_{12}O_{41}$: 3384.6360, found: 3386.6339 [M+H]$^+$; m/z calcd for $C_{185}H_{220}N_{10}O_{40}$: 3221.5483, found: 3221.5458 [M-isoxazoline]$^+$.

Compound 2i: The synthesis was performed according to modified procedure[35] with **1** (30 mg, 0.034 mmol) dissolved in toluene (50 mL) together with CBr$_4$ (1.128 g, 3.401 mmol). Subsequently, malonate **i** (348 mg, 0.340 mmol) dissolved in Freon 113/toluene 1:1 was added. After 15 min, DBU (101 µL, 0.68 mmol) dissolved in toluene (1 mL) was added over 45 min and the reaction mixture was stirred for additional 24 h. The crude product was plug-filtered and purified by column chromatography twice (SiO$_2$; Freon113/ethyl acetate/toluene/MeOH 5:5:1:1) to obtain **2i** as an orange solid (165 mg, 0.027 mmol, 79%). The product contained a fluorinated impurity (* in Figure S20 Supporting Information) identified as 4-(dimethylamino)-1-(2-(4,4,5,5,6,6,7,7,8,8,9,9,10,10,11,11,11-hep-

tadecafluoroundecyl- oxy)-2-oxoethyl)pyridinium that can be easily eliminated by washing with diluted HCl or by sublimation. This mixture was used without further purification to prepare the [5:0] pentakisadduct **3i** which was more easily purified afterwards. R_f (Freon 113:ethyl acetate:toluene:MeOH, 5:5:1:1) = 0.56; ^{1}H NMR (400 MHz, CDCl$_3$, rt): δ = 7.83 (d, J = 8.8 Hz, 2 H, H_{ortho}), 6.85–6.67 (m, 2 H, H_{meta}), 4.82–4.18 (m, 20 H, OCH_2), 3.14, 3.11 (s, 6 H, N(CH_3)$_2$), 2.62–1.85 (m, 20 H, CH_2), 1.82–1.02 ppm (m, 20 H, CH_2); MS (MALDI-TOF, dctb): m/z = 5836.78 [M-isoxazoline]$^+$, 6019.93 [M+Na]$^+$.

General procedure for isoxazolino deprotection—Synthesis of [5:0] pentakisadducts (3a–i)

The corresponding [5:1] hexakisadduct (1 equiv.) was dissolved in dry toluene ($\approx 1.5 \times 10^{-3}$ M) together with maleic anhydride (30 equiv.) under nitrogen atmosphere. The mixture was irradiated with a halogen flood light (500 W) while being cooled at 15 °C for 20–24 h. The mixture was filtered through silica plug and subsequently purified by column chromatography when needed.

Compound 3a:[14] The protected fullerene **2a** (75 mg, 0.045 mmol) was dissolved in dry toluene (30 mL) together with maleic anhydride (134 mg, 1.35 mmol). The mixture was purified by silica plug (toluene/ethyl acetate 95:5) to obtain pentakisadduct **3a** (43 mg, 0.028 mmol, 63%) as an orange solid which was further precipitated from CH$_2$Cl$_2$ into pentane. R_f (toluene:ethyl acetate 95:5) = 0.19; ^{1}H NMR (400 MHz, CDCl$_3$, rt): δ = 4.47–4.30 (m, 16 H, CH_2), 4.25 (q, J = 7.1 Hz, 4 H, CH_2), 1.42–1.32 (m, 24 H, CH_3), 1.26 ppm (t, J = 7.1 Hz, 6 H, CH_3); ^{13}C NMR (100 MHz, CDCl$_3$, rt): δ = 164.18, 164.06, 163.53, (10C, CO), 148.74, 147.13, 146.29, 145.94, 145.30, 144.81, 144.49, 144.42, 144.25, 143.33, 142.54, 140.04, 139.93 (50C, C$_{60}$-sp^2), 70.06, 69.63, 69.53, 69.30 (10C, C$_{60}$-sp^3), 63.12, 63.10, 62.88 (10C, CH$_2$), 54.05, 45.78, 45.10 (5C, COCCO), 14.22, 14.16, 14.14, 14.04 ppm (10C, CH$_3$); MS (MALDI-TOF, dctb): m/z = 1511.2803 [M]$^+$; IR (ATR, rt): $\tilde{v}$ = 2355, 1745, 1369, 1258, 1220, 1080, 1012 cm^{-1}.

Compound 3b: According to the general procedure for deprotection, fullerene **2b** (78 mg, 0.035 mmol) was irradiated in presence of maleic anhydride (89 mg, 1.00 mmol) in toluene (20 mL). The crude was purified by a silica plug with toluene to obtain **3b** as orange oil (46 mg, 0.022 mmol, 63%). R_f (toluene) = 0.12; ^{1}H NMR (400 MHz, CDCl$_3$, rt): δ = 4.44–4.21 (m, 16 H, OCH_2), 4.16 (t, J = 6.8 Hz, 4 H, OCH_2), 1.83–1.56 (m, 20 H, OCH$_2$CH_2), 1.47–1.16 (m, 60 H, CH_2), 0.99–0.78 ppm (m, 30 H, CH_3); ^{13}C NMR (100.5 MHz, RT, CDCl$_3$): δ = 164.13, 164.05, 164.00, 163.49 (10C, CO), 148.66, 147.04, 146.27, 145.86, 145.22, 144.71, 144.39, 144.33, 144.25, 143.24, 142.60, 139.95, 139.91 (50C, C$_{60}$-sp^2), 77.41, 77.16, 76.91, 70.18, 69.74, 69.64, 69.43 (10C, C$_{60}$-sp^3), 67.24, 67.01 (10C, OCH$_2$), 54.29, 46.01, 45.37 (5C, OCCCO), 31.53, 31.48 (10C, CH$_2$), 29.85, 28.65, 28.59, 28.48 (10C, CH$_2$), 25.74, 25.68, 25.59 (10C, CH$_2$), 22.69, 22.64 (10C, CH$_2$), 14.17 ppm (10C, CH$_3$); MS (MALDI-TOF, dctb): m/z = 2072 [M]$^+$; HRMS (APPI): m/z calcd for C$_{135}$H$_{130}$O$_{20}$: 2070.9155, found: 2071.9171 [M+H]$^+$; IR (ATR, rt): $\tilde{v}$ = 2956, 2928, 2858, 2364, 2336, 2160, 1747, 1467, 1255, 1215, 1080, 718, 527 cm^{-1}; UV/Vis (octanol): ε (λ_{max}) = 111 117 (211), 82 101 (244), 71 066 (282) M^{-1} cm^{-1} (nm).

Compound 3c: According to the general procedure for deprotection, fullerene **2c** (50 mg, 0.013 mmol) was irradiated in presence of maleic anhydride (37 mg, 0.383 mmol) in toluene (10 mL). The crude was purified by a silica plug with hexane/CH$_2$Cl$_2$ 2:1 to obtain **3c** (35 mg, 9.4 µmol, 72%) as an orange waxy solid. R_f (hexane:DCM, 2:1) = 0.28; ^{1}H NMR (400 MHz, CDCl$_3$, rt): δ = 4.30 (m, 16 H, OCH_2), 4.15 (t, J = 6.7 Hz, 4 H, OCH_2), 1.90–1.53 (m, 20 H, OCH$_2$CH_2), 1.42–1.17 (m, 300 H, CH_2), 0.87 ppm (t, J = 6.7 Hz, 30 H, CH_3); ^{13}C NMR (100.5 MHz, CDCl$_3$, rt): δ = 164.14, 164.05, 164.01, 163.49, 163.43 (10C, CO), 148.62, 147.03, 146.33, 145.87, 145.22,

144.73, 144.36, 144.29, 144.23, 143.25, 142.64, 139.90 (50C, C$_{60}$-sp^2), 70.16, 69.73, 69.62, 69.41, 68.92, 68.92, 67.39, 67.26, 67.20, 67.03 (10C, OCH$_2$ and 10C, C$_{60}$-sp^3), 54.24, 50.97, 45.95, 45.32 (5C, OCCCO), 32.10, 32.09, 32.08, 32.08, 29.91, 29.90, 29.89, 29.86, 29.83, 29.81, 29.79, 29.76, 29.73, 29.70, 29.62, 29.53, 29.52, 29.44, 29.41, 29.26, 28.71, 28.66, 28.63, 28.55, 28.37, 26.10, 26.06, 26.03, 25.97, 25.75, 22.85 (160C, CH$_2$), 14.27 ppm (10C, CH$_3$); MS (MALDI-TOF, dctb): m/z 3756.95 [M+H]$^+$, 3778.87 [M+Na]$^+$ and 3794.81 [M+K]$^+$; HRMS (APPI): m/z calcd for C$_{255}$H$_{371}$O$_{20}$: 3753.7969, found: 3753.8008 [M+H]$^+$; IR (ATR, rt): $\tilde{v}$ = 2910, 2844, 2154, 1745, 1464, 1249, 1199, 1067 cm^{-1}; UV/Vis (octanol): ε (λ_{max}) = 106 287 (211), 75 586 (244), 62 986 (211) M^{-1} cm^{-1} (nm).

Compound 3d: According to the general procedure for deprotection, fullerene **2d** (60 mg, 0.028 mmol) was irradiated in presence of maleic anhydride (83 mg, 0.844 mmol) in toluene (25 mL). The mixture was purified by silica plug (toluene/ethyl acetate 9:1) and subsequently purified by column chromatography to obtain pentakisadduct **3d** (52 mg, 0.025 mmol, 87%) as an orange solid which was further precipitated from CH$_2$Cl$_2$ into pentane. R_f (toluene:ethyl acetate 9:1) = 0.66; ^{1}H NMR (400 MHz, CDCl$_3$, rt): δ = 7.40–7.14 (m, 50 H, Ph), 5.40–5.10 ppm (m, 20 H, OCH_2Ph); ^{13}C NMR (100.5 MHz, CDCl$_3$, rt): δ = 163.85, 163.81, 163.72, 163.24 (10C, CO), 146.91, 146.07, 145.75, 145.12, 144.63, 144.41, 144.04, 143.80, 143.10, 142.06, 139.61, 139.49 (50C, C$_{60}$-sp^2), 134.78, 134.67 (10C, C$_{ipso}$ Ph), 129.11, 129.05, 128.97, 128.88, 128.81, 128.76, 128.69 (50C, CH-Ph), 69.06, 68.82, 68.78, 68.61 (10C, C$_{60}$-sp^3), 53.66, 52.03 ppm (5C, OCCCO); MS (MALDI-TOF, dctb): m/z = 2131.31 [M]$^+$; IR (ATR, rt): $\tilde{v}$ = 2949, 2182, 1745, 1497, 1447, 1370, 1254, 1210, 1066, 978, 741 cm^{-1}.

Compound 3e: According to the general procedure for deprotection, fullerene **2e** (65 mg, 0.021 mmol) was irradiated in presence of maleic anhydride (61 mg, 0.630 mmol) in toluene (25 mL). The crude product was plug-filtered (SiO$_2$; toluene → toluene/CHCl$_3$ 1:1 → CHCl$_3$ 3% vol. pyridine) and purified twice by column chromatography (SiO$_2$; CHCl$_3$ 3% vol. pyridine) to yield **3e** (38 mg, 0.014 mmol, 67%) as an orange viscous oil. R_f (EtOAc 3% py) = 0.61; ^{1}H NMR (400.05 MHz, CDCl$_3$, rt): δ = 7.19–6.89 (m, 20 H, CH-Ar), 6.81–6.50 (m, 20 H, CH-Ar), 4.66–4.03 (m, 20 H, OCH_2), 3.08–2.63 ppm (m, 80 H, CH_2 and N(CH_3)$_2$); ^{13}C NMR (75 MHz, CDCl$_3$, rt): δ = 167.75, 163.92, 162.44 (10C, CO), 149.60, 147.89, 146.97, 145.93, 145.15, 144.32, 143.29, 142.56, 139.91, (50C, C$_{60}$-sp^2 and 10C, C-N(CH$_3$)$_2$, 132.18, 130.33, 129.82, 129.73, 129.69, 126.52, 125.18, 122.82, 113.99, 113.35, 113.18, 111.85 (50C, Ar), 69.42, 68.85, 67.86, 66.77, 64.08, 63.57 (10C, OCH$_2$), 41.00, 40.92, 38.64, 38.32 (20C, N(CH$_3$)$_2$), 35.95, 34.08, 33.93, 32.06 ppm (10C, CH$_2$-Ar); MS (MALDI-TOF, dhb): m/z = 2702.99 [M]$^+$, 2725.97 [M+Na]$^+$, 2742.94 [M+K]$^+$; IR (ATR, rt): $\tilde{v}$ = 2932, 2347, 1745, 1612, 1525, 1453, 11 348, 1232, 1160, 1045, 945, 807, 735 cm^{-1}.

Compound 3f: According to the general procedure for deprotection, fullerene **2f** (45 mg, 0.014 mmol) was irradiated in presence of maleic anhydride (40 mg, 0.410 mmol) in toluene (12 mL). The crude product was purified by a silica plug (SiO$_2$; toluene/CH$_2$Cl$_2$/MeOH 4:5:1) and purified twice by column chromatography (SiO$_2$; toluene/CH$_2$Cl$_2$/MeOH 4:5:1) to yield **3f** (24.3 mg, 7.7 µmol, 55%) as an orange oil. R_f (toluene:DCM:MeOH, 5:4:1) = 0.22; ^{1}H NMR (400.05 MHz, CDCl$_3$, rt): δ = 4.57–4.27 (m, 20 H, COOCH_2), 3.89–3.46 (m, 140 H, OCH_2), 3.37 (s, 6 H, OCH_3), 3.36 (s, 18 H, OCH_3), 3.35 ppm (6 H, OCH_3); ^{13}C NMR (100.5 MHz, CDCl$_3$, rt): δ = 163.85, 163.82, 163.73, 163.21 (10C, CO), 148.72, 147.12, 146.34, 145.97, 145.28, 144.86, 144.51, 144.33, 144.09, 143.26, 142.44, 139.87, 139.82 (50C, C$_{60}$-sp^2), 72.03, 70.75, 70.69, 70.65, 70.61, 70.59 (110C, OCH$_2$), 69.89, 69.49, 69.47, 69.17, 68.73, 68.56, 66.07, 65.95, 65.81 (10C, C$_{60}$-sp^3), 59.14, 59.12 (10C, OCH$_3$), 45.53, 44.89 ppm (5C, COCCO); MS

(MALDI-TOF, dctb): $m/z = 3155.7231$ $[M+Na]^+$, 3172.6973 $[M+K]^+$; UV/Vis (octanol): ε $(\lambda_{max}) = 166\,616$ (211), 132 341 (244), 98 811 (282) $M^{-1}cm^{-1}$ (nm).

Compound 3g$_{-tBu}$:[14] According to the general procedure for deprotection, fullerene 2g$_{-tBu}$ (59 mg, 0.019 mmol) was irradiated in presence of maleic anhydride (57 mg, 0.572 mmol) in toluene (15 mL). The crude product was purified by a silica plug (SiO$_2$; toluene/ethyl acetate 9:1→8:2) and purified twice by column chromatography (SiO$_2$; toluene/ethyl acetate 9:1) to yield 3g$_{-tBu}$ (30.3 mg, 1.12 μmol, 59%) as an orange viscous oil. R_f (toluene:ethyl acetate, 9:1) = 0.2; ^{1}H NMR (400 MHz, CDCl$_3$, rt): $\delta = 4.50$–4.07 (m, 20H, OCH$_2$), 2.31–2.07 (m, 20H, CH$_2$CO), 1.84–1.52 (m, 20H, CH$_2$), 1.44, 1.43, 1.43, 1.42 (s, 90H, CH$_3$), 0.97–0.72 ppm (m, 20H, CH$_2$); ^{13}C NMR (100.5 MHz, CDCl$_3$, rt): $\delta = 173.07$, 173.06 (10C, COOtBu), 167.98, 164.12, 164.07, 164.00, 163.47 (10C, CO), 148.75, 147.13, 146.50, 145.97, 145.27, 144.84, 144.39, 144.29, 144.22, 143.32, 142.70, 139.91, 139.84 (50C, C$_{60}$-sp^2), 80.23, 80.19 (10C, C(CH$_3$)$_3$), 70.04, 69.65, 69.54, 69.33, 66.97, 66.90, 66.74, 66.33 (10C, C$_{60}$-sp^3 and 10C, OCH$_2$), 54.05, 45.75, 45.14 (5C, OCCCO), 35.42 (10C, CH$_2$CO), 29.78 (10C, CH$_2$), 28.31, 28.21 (30C, CH$_3$), 25.43, 25.33 (10C, CH$_2$), 24.72, 24.67 ppm (10C, CH$_2$); MS (MALDI-TOF, dctb): $m/z = 2933.78$ $[M]^+$; HRMS (APPI): m/z calcd for C$_{175}$H$_{190}$O$_{40}$: 2931.2828, found: 2931.2809 $[M]^+$; IR (ATR, rt): $\tilde{v} = 1726$, 1609, 1456, 1392, 1366, 1218, 1150, 1069, 848 cm^{-1}; UV/Vis (octanol): ε $(\lambda_{max}) = 124\,919$ (211), 88 744 (244), 72 568 (282) $M^{-1}cm^{-1}$ (nm).

Compound 3h$_{-BOC}$:[14] According to the general procedure for deprotection, fullerene 2h$_{-BOC}$ (90 mg, 0.026 mmol) was irradiated in presence of maleic anhydride (78 mg, 0.797 mmol) in toluene (25 mL). The crude product was purified by a silica plug (SiO$_2$; toluene/THF, 10:0 to 8:2) and purified by column chromatography (SiO$_2$; toluene/THF, 9:1) to yield 3h$_{-BOC}$ (81 mg, 0.025 mmol, 96%) as an orange viscous oil. R_f (toluene:THF, 8:2) = 0.35; ^{1}H NMR (400 MHz, CDCl$_3$, rt): $\delta = 4.81$, 4.55 (bs, 10H, NH), 4.41–3.52 (m, 20H, OCH$_2$), 3.39–2.81 (m, 20H, CH$_2$NH), 2.04–1.46 (m, 40H, CH$_2$), 1.42 (s, 90H, CH$_3$), 1.39–0.69 ppm (m, 40H, CH$_2$); ^{13}C NMR (100.5 MHz, RT, CDCl$_3$, rt): $\delta = 167.65$, 164.18, 164.08, 163.55 (10C, CO), 156.34 (10C, COOtBu), 148.76, 148.74, 147.09, 146.30, 145.88, 145.20, 145.19, 144.77, 144.77, 144.76, 144.41, 144.36, 144.24, 143.31, 142.60, 139.95, (50C, C$_{60}$-sp^2), 79.28, 79.19, 79.16, 79.13 (10C, C(CH$_3$)$_3$), 70.08, 69.64, 69.58, 69.32, 67.76, 67.54, 67.24, 67.11, 67.10, 67.08, 66.91 (10C, C$_{60}$-sp^3), 62.75 (10C, OCH$_2$), 45.89, 45.26 (5C, OCCCO), 40.57, 40.42, 40.40 (10C, CH$_2$NH), 32.56, 32.36 (10C, CH$_2$), 30.09, 30.04, 30.01, 29.96, 29.68, 29.55 (10C, CH$_2$), 28.51, 28.47, 28.28 (30C, CH$_3$), 26.46, 26.43, 26.39, 25.93, 25.88, 25.70, 25.67, 25.65, 25.57, 25.28, 23.88, 23.57 ppm (20C, CH$_2$); HRMS (APPI): m/z calcd for C$_{185}$H$_{220}$N$_{10}$O$_{40}$: 3221.5483, found: 3221.5525 $[M]^+$; MS (MALDI-TOF, dctb): $m/z = 3234.67$ $[M+H]^+$; IR (ATR, rt): $\tilde{v} = 3349$, 2969, 2858, 2355, 1741, 1689, 1519, 1390, 1361, 1250, 1221, 1157, 1046, 988, 859, 748 cm^{-1}; UV/Vis (octanol): ε $(\lambda_{max}) = 98\,457$ (211), 66 536 (244), 52 850 (282) $M^{-1}cm^{-1}$ (nm).

Compound 3i: The synthesis was performed according to general procedure for deprotection with a modified solvent mixture. Fullerene 2i (165 mg, 0.027 mmol) was dissolved together with maleic anhydride (80 mg, 0.820 mmol) in Freon 113/toluene 1:1 (40 mL) and irradiated. The crude product was purified by short column chromatography (SiO$_2$ Freon113/toluene/CH$_2$Cl$_2$ 4:4:1→Freon113/toluene/MeOH 4:4:1) to obtain 3i (81 mg, 0.014 mmol, 51%) as an orange solid. R_f (toluene:Freon 113:DCM, 4:4:1) = 0.60; ^{1}H NMR (400 MHz, C$_6$D$_6$/C$_6$F$_6$ 1:1): $\delta = 4.85$–4.24 (m, 20H OCH$_2$), 2.65–1.96 (m, 40H, OCH$_2$CH$_2$CH$_2$) ppm; ^{19}F NMR (282 MHz, C$_6$D$_6$/C$_6$F$_6$ 1:1): $\delta = -79.16$ (t, $J_{FF}=9.9$ Hz, 30F, CF$_3$), −107.66, −108.40, −109.84 (bs), −111.99, −112.50 (s), −114.05, −116.60—−117.22 (m), −118.47—−119.59 (m), −119.76—−120.33 (m), −120.48 (bs), −123.73 (bs),

−129.03, −129.17, −137.81 (dd, $J=15.7$, 5.5 Hz), −139.82 ppm (m); ^{13}C NMR (100.5 MHz, C$_6$D$_6$/C$_6$F$_6$ 1:1): $\delta = 90.17$–89.06 (m), 87.47–86.65 (m), 60.97, 60.73, 60.49 (10C, OCH$_2$), 50.87, 48.40 (10C, CH$_2$CF$_2$), 15.10 ppm (10C, CH$_2$CH$_2$CH$_2$), Fullerene signals could not be detected; MS (MALDI-TOF, dctb): $m/z = 5838.27$ $[M+H]^+$; IR (ATR, rt): $\tilde{v} = 2921$, 2849, 2171, 1740, 1458, 1370, 1332, 1194, 1138, 1122, 1028, 972, 801, 735, 696, 646 cm^{-1}. UV/vis (C$_2$Cl$_3$F$_3$): ε $(\lambda_{max}) = 120\,316$ (244), 93 735 (282) $M^{-1}cm^{-1}$ (nm).

Synthesis of [5:0] fullerenes bearing ionizable groups

General procedure for deprotection—Synthesis of [5:0] pentakisadducts (3g,h)

The deprotections were carried out following a modified protocol from literature.[11b]

Compound 3g: Pentakisadduct 3g$_{-tBu}$ (20 mg, 6.8 μmol) was dissolved in CH$_2$Cl$_2$/TFA 4:1 mixture (2 mL) and the solution was stirred overnight at room temperature. Remaining TFA was removed under vacuum and co-evaporated with toluene/MeOH several times to give 3g as an orange waxy solid. ^{1}H NMR (400 MHz, CD$_3$OD, rt): $\delta = 4.56$–4.10 (m, 20H, OCH$_2$), 2.49–2.09 (m, 20H, CH$_2$COOH), 1.89–1.31 ppm (m, 60H, (CH$_2$)$_3$); ^{13}C NMR (100.5 MHz, CD$_3$OD, rt): $\delta = 177.46$, 175.85 (10C, COOH), 165.09, 164.88 (10C, CO), 149.91, 148.17, 144.48, 143.87, 141.45, 133.69, 132.49, 130.00 (50C, C$_{60}$-sp^2), 71.00, 70.72 (10C, C$_{60}$-sp^3), 68.30, 68.20, 68.11, 67.98 (10C, OCH$_2$), 34.79, 34.76, 34.71 (10C, CH$_2$COOH), 30.73, 29.45, 29.39, 29.29, 26.71, 26.67, 25.66, 25.59, 25.36 ppm (30C, CH$_2$), 5C for COCCO are probable hidden under the solvent peak and were not observable; HRMS (ESI, negative): m/z calcd for C$_{135}$H$_{110}$O$_{40}$: 2370.6573 (not detected); calcd for C$_{135}$H$_{108}$O$_{40}^{2-}$ $[M$-2H]$^{2-}$: 1184.8221, found: 1184.8224; IR (ATR, rt): $\tilde{v} = 1678$, 1410, 1256, 1198, 942, 799, 731 cm^{-1}; UV/Vis (H$_2$O pH7.0, 0.5 M phosphate buffer): ε $(\lambda_{max}) = 68\,287$ (211), 57 812 (244), 48 897 (282) $M^{-1}\cdot cm^{-1}$ (nm)

Compound 3h: Pentakisadduct 3h$_{-BOC}$ (35 mg, 0.01 mmol) was dissolved in CH$_2$Cl$_2$/TFA 4:1 mixture (4 mL) and the solution was stirred overnight at room temperature. Remaining TFA was removed under vacuum and co-evaporated with toluene/MeOH several times to give 3h (14 mg, 0.006 mmol, 60%) as an orange solid. ^{1}H NMR (400 MHz, CD$_3$OD, rt): $\delta = 6.81$ (b.s., NH$_3^+$), 3.43–2.97 (m, 20H, OCH$_2$), 1.90–1.74 (m, 20H, CH$_2$N), 0.84–0.08 ppm (m, 80H; CH$_2$); ^{13}C NMR (100.5 MHz, CD$_3$OD, rt): $\delta = 167.54$, 165.05, 164.94, 164.87, 164.43 (10C, CO), 163.96–161.93 (m, 10C, COOCF$_3$), 149.92, 148.14, 147.03, 146.82, 146.21, 145.94, 145.77, 145.67, 145.61, 144.50, 143.78, 141.52, 141.43, (50C, C$_{60}$-sp^2), 134.76, 133.59 (m), 131.92, 130.45, 120.11, 119.19 (m), 117.54, 117.30–116.22 (m), 114.71 (10C, COOCF$_3$), 71.69, 71.07, 70.95, 70.72, 69.31, 68.34, 68.16, 66.06, 64.91 (10C, C$_{60}$-sp^3), 62.68 (10C, OCH$_2$), 47.91, 47.33 (5C, COCCO), 40.61, 33.22 (10C, CH$_2$N), 29.41, 29.34, 29.28, 29.17, 28.91, 28.50, 28.45, 28.37, 28.34, 27.18, 27.00, 26.91, 26.86, 26.56, 26.49, 26.43, 26.39, 26.12 ppm (40C, CH$_2$); MS (MALDI-TOF, dhb): $m/z = 2222.12$ $[M+H]^+$, 2246.14 $[M+Na]^+$; IR (ATR, rt): $\tilde{v} = 2494$, 1643, 1431, 1203 cm^{-1}; UV/Vis (H$_2$O pH7.0, 0.5 M phosphate buffer): ε $(\lambda_{max}) = 39\,381$ (282) $M^{-1}cm^{-1}$ (nm).

Conflict of interest

The authors declare no conflict of interest.

[1] A. Hirsch, *Nat. Mater.* **2010**, *9*, 868–871.
[2] a) A. M. Lopez, A. Mateo-Alonso, M. Prato, *J. Mater. Chem.* **2011**, *21*, 1305–1318; b) W. Yan, S. M. Seifermann, P. Pierrat, S. Bräse, *Org. Biomol. Chem.* **2015**, *13*, 25–54.
[3] A. Hirsch, J. M. Englert, F. Hauke, *Acc. Chem. Res.* **2013**, *46*, 87–96.
[4] H. Hoppe, N. S. Sariciftci, *J. Mater. Chem.* **2006**, *16*, 45–61.
[5] V. M. Torres, M. Posa, B. Srdjenovic, A. L. Simplício, *Colloids Surf. B* **2011**, *82*, 46–53.
[6] a) J.-N. Wang, Y.-L. Zhang, Y. Liu, W. Zheng, L. P. Lee, H.-B. Sun, *Nanoscale* **2015**, *7*, 7101–7114; b) Y. Li, J. Yang, Q. Zhao, Y. Li, *Langmuir* **2013**, *29*, 13527–13534.
[7] A. B. Marco, D. Cortizo-Lacalle, I. Perez-Miqueo, G. Valenti, A. Boni, J. Plas, S. Strutyński, S. De Feyter, F. Paolucci, M. Montes, *Angew. Chem. Int. Ed.* **2017**, *56*, 6946–6951; *Angew. Chem.* **2017**, *129*, 7050–7055.
[8] J. M. Englert, J. Röhrl, C. D. Schmidt, R. Graupner, M. Hundhausen, F. Hauke, A. Hirsch, *Adv. Mater.* **2009**, *21*, 4265–4269.
[9] V. León, M. Quintana, M. A. Herrero, J. L. Fierro, A. de la Hoz, M. Prato, E. Vázquez, *Chem. Commun.* **2011**, *47*, 10936–10938.
[10] I. Rašović, *Mater. Sci. Technol.* **2017**, *33*, 777–794.
[11] a) J.-F. Nierengarten, *New J. Chem.* **2004**, *28*, 1177–1191; b) F. Hörmann, A. Hirsch, *Chem. Eur. J.* **2013**, *19*, 3188–3197; c) L. K. Wasserthal, A. Krat-zer, A. Hirsch, *Eur. J. Org. Chem.* **2013**, 2355–2361.
[12] F. Langa, P. de la Cruz, A. Espíldora, A. González-Cortés, A. de la Hoz, V. López-Arza, *J. Org. Chem.* **2000**, *65*, 8675–8684.
[13] T. Wei, M. E. Perez-Ojeda, A. Hirsch, *Chem. Commun.* **2017**, *53*, 7886–7889.
[14] F. Hörmann, W. Donaubauer, F. Hampel, A. Hirsch, *Chem. Eur. J.* **2012**, *18*, 3329–3337.
[15] X. Camps, A. Hirsch, *J. Chem. Soc. Perkin Trans. 1* **1997**, 1595–1596.
[16] F. Hörmann, M. Brettreich, W. Donaubauer, F. Hampel, A. Hirsch, *Chem. Eur. J.* **2013**, *19*, 2814–2825.
[17] A. Hirsch, I. Lamparth, T. Grösser, H. R. Karfunkel, *J. Am. Chem. Soc.* **1994**, *116*, 9385–9386.
[18] G. Wen, Z. Guo, W. Liu, *Nanoscale* **2017**, *9*, 3338–3366.
[19] H. Asanuma, H. Li, T. Nakanishi, H. Möhwald, *Chem. Eur. J.* **2010**, *16*, 9330–9338.
[20] J. Zhang, J. Li, Y. Han, *Macromol. Rapid Commun.* **2004**, *25*, 1105–1108.
[21] C. Hansch, A. Leo, S. H. Unger, K. H. Kim, D. Nikaitani, E. J. Lien, *J. Med. Chem.* **1973**, *16*, 1207–1216.
[22] S. R. Holmes-Farley, C. D. Bain, G. M. Whitesides, *Langmuir* **1988**, *4*, 921–937.
[23] Y. Tajima, T. Matsuura, Y. Numata, D. Yamazaki, H. Kawamura, H. Osedo, *Jpn. J. Appl. Phys.* **2008**, *47*, 5730.
[24] C. T. Jafvert, P. P. Kulkarni, *Environ. Sci. Technol.* **2008**, *42*, 5945–5950.
[25] C. Richardson, D. Schuster, S. Wilson in *Fullerenes 2000 Vol. 9 Functional-ized Fullerenes: Proceedings of the International Symposium* (Eds.: N. Martin, M. Maggini, D. M. Guldi), The Electrochemical Society, Penning-ton, NJ, USA, **2000**, p. 226.
[26] H. Murakami, Y. Watanabe, N. Nakashima, *J. Am. Chem. Soc.* **1996**, *118*, 4484–4485.
[27] a) L. Wasserthal, B. Schade, K. Ludwig, C. Böttcher, A. Hirsch, *Chem. Eur. J.* **2014**, *20*, 5961–5966; b) Z. Lin, P. Lu, C.-H. Hsu, K. Yue, X.-H. Dong, H. Liu, K. Guo, C. Wesdemiotis, W.-B. Zhang, X. Yu, S. Z. D. Cheng, *Chem. Eur. J.* **2014**, *20*, 11630–11635; c) Y. Zhao, G. Chen in *C60 Fullerene Am-phiphiles as Supramolecular Building Blocks for Organized and Well-De-fined Nanoscale Objects* (Ed.: J.-F. Nierengarten), Springer, Berlin, Heidel-berg, **2014**, pp. 23–53.
[28] a) N. Tirelli, F. Cardullo, T. Habicher, U. W. Suter, F. Diederich, *J. Chem. Soc. Perkin Trans. 2* **2000**, 193–198; b) X. Zhang, B. Yu, H. Cong, *Curr. Org. Chem.* **2017**, *21*, 1600–1611.
[29] a) H. Murakami, T. Nakanishi, M. Morita, N. Taniguchi, N. Nakashima, *Chem. Asian J.* **2006**, *1*, 860–867; b) D. Felder, M. D. P. Carreón, J.-L. Gal-lani, D. Guillon, J.-F. Nierengarten, T. Chuard, R. Deschenaux, *Helv. Chim. Acta* **2001**, *84*, 1119–1132; c) M. Hetzer, T. Gutberlet, M. F. Brown, X. Camps, O. Vostrowsky, H. Schönberger, A. Hirsch, T. M. Bayerl, *J. Phys. Chem. A* **1999**, *103*, 637–642; d) T. Nakanishi, W. Schmitt, T. Michinobu, D. G. Kurth, K. Ariga, *Chem. Commun.* **2005**, 5982–5984; e) S. S. Gaya-thri, A. K. Agarwal, K. A. Suresh, A. Patnaik, *Langmuir* **2005**, *21*, 12139–12145.
[30] T. Homma, K. Harano, H. Isobe, E. Nakamura, *J. Am. Chem. Soc.* **2011**, *133*, 6364–6370.
[31] J.-M. Janot, E. Bienvenue, P. Seta, R. V. Bensasson, A. C. Tome, R. F. Enes, J. A. S. Cavaleiro, S. Leach, X. Camps, A. Hirsch, *J. Chem. Soc. Perkin Trans. 2* **2000**, 301–306.
[32] H. Li, S. A. Haque, A. Kitaygorodskiy, M. J. Meziani, M. Torres-Castillo, Y.-P. Sun, *Org. Lett.* **2006**, *8*, 5641–5643.
[33] K. O. Siegenthaler, A. Schäfer, A. Studer, *J. Am. Chem. Soc.* **2007**, *129*, 5826–5827.
[34] P. Witte, F. Hörmann, A. Hirsch, *Chem. Eur. J.* **2009**, *15*, 7423–7433.
[35] S. R. Wilson, M. E. Yurchenko, D. I. Schuster, E. N. Yurchenko, O. Sokolo-va, S. E. Braslavsky, G. Klihm, *J. Am. Chem. Soc.* **2002**, *124*, 1977–1981.
[36] M. Braun, U. Hartnagel, E. Ravanelli, B. Schade, C. Boettcher, O. Vostrow-sky, A. Hirsch, *Eur. J. Org. Chem.* **2004**, 1983–2001.